31st Annual International Conference of the IEEE EMBS
Minneapolis, Minnesota, USA, September 2-6, 2009

Multiphoton Autofluorescence Microscopy and Second Harmonic Generation Microscopy of Oral Epithelial Neoplasms

Gracie Vargas, Tuya Shilagard, Ki-Hong Ho, Susan McCammon

Abstract—: **The objective of this study was to evaluate the nonlinear optical microscopy techniques of multiphoton autofluorescence microscopy (MPAM) and second harmonic generation microscopy (SHGM) for noninvasive imaging of oral epithelial carcinogenesis. In vivo imaging was performed in a hamster model for oral carcinogenesis to characterize optical and morphometric alterations during neoplastic transformation. Data is presented showing alterations in morphometry and collagen density during the precancerous phase of neoplastic transformation.**

I. Introduction

THE majority (96%) of oral cancers are epithelial squamous cell carcinomas (SCC), which are characterized by invasion of submucosal connective tissue by overlying strands, sheets, or islands of neoplastic epithelial cells [1]. SCC is preceded by premalignant lesions (hyperplasia, dysplasia) that are traditionally identified by visual white light inspection [2]. White light inspection is sufficient for detecting gross morphological changes on the tissue surface. However, since microstructural alterations indicative of transformation cannot be assessed below the surface, it cannot be used to differentiate between the diversity of benign lesions, precancers (hyperplasia, leukoplakia), benign inflammation, or carcinoma-in-situ. Biopsy of every morphologically abnormal region is impractical, so often a suspicious-looking area is followed over time, visually or by surveillance biopsy [2]. Once a biopsy is taken, that same tissue section is unavailable for future study and biopsies can only be taken from neighboring regions. Thus, the ability to follow the multi-step process of carcinogenesis is limited to single timepoints. The ability to evaluate the oral mucosa at the microscopic level in vivo over time would greatly enhance our understanding of the timecourse of premalignant/malignant transformation and would be helpful in the development of more effective diagnostic and treatment approaches.

Previous efforts to image the oral mucosa by nonlinear optical microscopies have ranged from the optical and microstructural characterization of normal oral mucosa to feasibility studies evaluating these techniques for their diagnostic potential. Sun et al. combined MPAM with SHGM to reveal microstructural and spectroscopic features of normal oral mucosa in the hamster buccal pouch [3],[4]. Wilder-Smith et al. used MPAM for in vivo imaging of the transformed hamster buccal pouch and based on comparison with histological scores determined relatively high levels of agreement by Kappa statistics [5]. In a similar study, Skala et al. tested the diagnostic potential of MPAM on upper epithelium of *ex vivo* tissue biopsies taken from hamster buccal pouch SCC model [6]. The study demonstrated statistically significant changes in cellular morphology and autofluorescence between normal and abnormal samples. Neither of the latter two studies made direct comparisons to corresponding histology to correlate MPM signals to microstructural parameters. In the current study MPAM and SHGM imaging are combined for *in vivo* imaging of malignant transformation in an animal model for oral cancer to depths that include both the epithelium and stroma. The source of MPA is from endogenous fluorophores in the epithelium and stroma whereas the SHG signal arises from fibrillar collagen, which is located in the stroma [3]. Fibrillar collagen has been shown to give rise to SHG [7].

II. Methods

A. Animal Model for oral carcinogenesis

A Golden Syrian hamster model for oral precancers and squamous cell carcinoma (SCC) was utilized in this study. Briefly, carcinogenesis was induced in the buccal pouch of Syrian Golden hamsters by trice-weekly application of 0.5% 9,10-dimethyl-1,2-benzanthracene (DMBA). This model closely mimics the stages of precancers and squamous cell carcinoma in humans both in its histology and in the expression of key molecular biomarkers. [7][8]. A typical timeline for premaligant and malignant transformation following initiation of the thrice-weekly DMBA painting is as follows: hyperkeratosis is present within two weeks, followed by evidence of mild dysplasia as early as 3-5 weeks, moderate to high-grade dysplasia/carcinoma-in-situ within 4-8 weeks, and SCC is generally evident beyond 8-12 weeks. The left buccal pouch served as an age-control, since previous studies indicated that DMBA painting of the right pouch does not alter the left control pouch.

B. Imaging

In vivo images were obtained via the MPM system as previously described [3][4]. The system utilizes a

Manuscript received April 23, 2009. This work was supported in part by the National Institutes of Health under Grant R01CA127429-01 and the John Sealy Memorial Endowment Fund under Grant 6074-03.

G. Vargas is with the University of Texas Medical Branch (phone: 409-772-7214; fax: 409-772-0751; e-mail: grvargas@ utmb.edu).

Ti:sapphire laser (Tsunami, Spectra Physics) with a 5W frequency-doubled Nd:YVO4 pump for the excitation source. Typical pulse width at the sample (after the objective) is 140 fs with an 80 MHz repetition rate. Average power at the sample is 20 mW. The objective used in these studies is a long working distance water immersion objective (Zeiss, 40X, 0.8 NA). Nondecanned detection was performed using cooled photomultiplier tubes.

Prior to imaging hamsters were anesthetized using a Ketamine (100mg/kg)/Xylazine (10mg/kg) mixture given IP. The hamster buccal pouch was pulled out of the oral cavity and retained on a flat sample holder with care being taken not to stretch the tissue. The hamster was placed on the x-y stage of the inverted microscope with the buccal sample holder centered over the objective. Regions of interest to be imaged were first identified using a 10X 0.3 NA objective having a 1.2 mm field of view. The objective turret was then rotated to the 40X objective for obtaining high resolution z-stacks using a pixel dwell time of 30 µs. A no. 1.5 coverslip was used on all samples. A z-stack was obtained using a z-interval of 1 µm to depths of 150-200 µm. Illumination was at 800 nm, with broadband emission collected at 450-650 µm, and SHG collected using a 400(14)nm filter.

In single timepoint imaging, biopsies (1 mm) were obtained of the imaged areas. Quadrant markings on the buccal pouch made by India ink in areas far from imaging combined with observation of vascular patterns on the buccal pouch were helpful in obtaining biopsies from imaged areas. Longitudinal imaging was performed by imaging the same site over a seven week period when dysplasia is evident throughout the pouch. No biopsies were obtained until after the final week, at which time a 1mm biopsy was obtained of the imaged areas and processed for histology. Imaging and biopsies were taken from the control side of the buccal pouch in the same general area as in the experimental pouch.

Image stacks were analyzed for changes in volume of sampled region that had a positive SHG signal relative to total volume of the imaged stack. This was performed by analysis of only the first 50 µm of the stromal tissue (obtained from the SHG z-stack) – SHG relative volume metric was determined by thresholding the reconstructed volume and determining voxels that were positive for SHG signal compared to total volume.

III. Results

Typical MPAM micrographs in the *in vivo* normal oral mucosa are shown in Fig. 1, where cross-sectional MPAM akin to the typical view of histology is shown along with x-y micrographs taken from various depths. These cross-sectional views are particularly appropriate since they provide a representation that is more akin to histological sections used by pathologists for diagnosing epithelial neoplastic transformation. In the normal case, there is a thin keratinizing layer with well defined keritinocytes followed by a regular epithelial layer (only one slice is shown), and a highly collagenous stromal layer.

A sample after four weeks treatment with DMBA is shown in Fig. 2. In this case the keratin layer is thickened and less regular than in the normal control. Keratinocytes are not regularly shaped/spaced as in the normal control. Dysplastic cells can be identified in the epithelial x-y micrograph labeled epithelium. Stromal collagen appears less defined as well.

In longitudinal imaging studies, there was an increase in thickness of all epithelial layers with significance occurring after three weeks (data not shown). In the stroma, SHG relative volume analysis indicated an initial increase in collagen volume after three weeks followed by subsequent and large decrease by seven weeks when dysplasia is common throughout (Fig. 3).

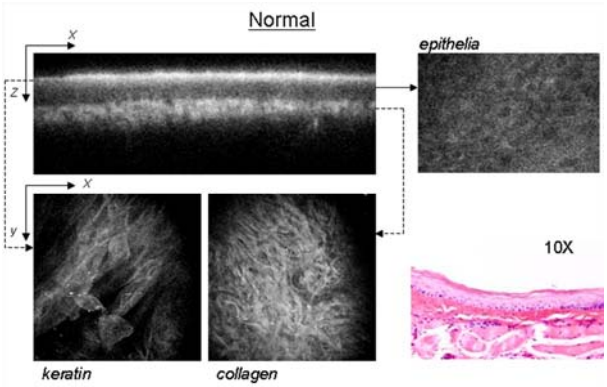

Fig. 1. Typical MPAM micrographs from normal in vivo oral mucosa. Top left panel: cross-sectional view showing layered structure of the mucosa. Accompanying panels show x-y micrographs of the surface keratinizing layer (keratin), underlying epithelial cells (epithelium), and the stroma (collagen). The corresponding H&E obtained from a biopsy of the tissue after in vivo imaging is also shown.

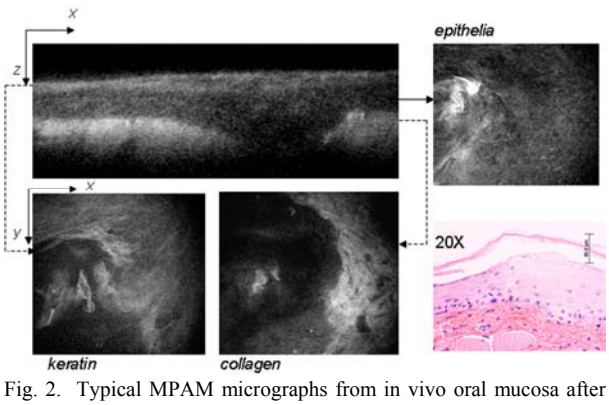

Fig. 2. Typical MPAM micrographs from in vivo oral mucosa after DMBA treatment. Top left panel: cross-sectional view showing layered structure of the mucosa. Accompanying panels show x-y micrographs of the surface keratinizing layer (keratin), underlying dysplastic epithelial cells (epithelium), and the stroma (collagen). The corresponding H&E obtained from a biopsy of the tissue after in vivo imaging is also shown.

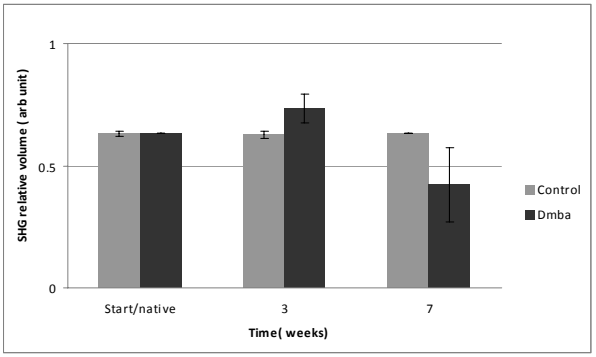

Fig. 3. Changes in stromal collagen relative volume based on volume of tissue positive for SHG signal. A significant increase is noted by three weeks in the DMBA treated sample, followed by a decrease after seven seeks. No change was found in the untreated controls (n=4)

IV. Discussion

This work is an extension of our previous work to characterize the normal oral mucosa and the work of others to assess the potential of nonlinear optical microscopy for diagnostic differentiation of neoplastic transformation. Our results indicate that MPAM-SHGM is capable of elucidating morphometric alterations early in the multi-step process of malignant transformation. This combined with detection of spectroscopic alterations can lead to MPM-SHGM serving as a powerful adjunct to surveillance biopsy of epithelial tissues.

This study explores MPAM and SHGM imaging of the full epithelium and upper stroma. This allows for features of both the epithelium and stroma to be assessed revealing spectroscopic and morphometric features of both layers affected by transformation. Longitudinal imaging allows for enhanced understanding of neoplastic transformation, particularly when coupled with biological examination as will be performed in future studies. In the current study there was an interesting trend in which relative volume having SHG increased within three weeks over the control and subsequently decreased. The source of SHG in the stroma is most likely due to Type I which makes a significant portion of this subepithelial layer. Changes in stromal architecture including proteolytic degradation of collagen modulated by collagenases during transformation are known to occur. However specific time resolved alterations are not elucidated and current studies are underway to correlate the time course of SHG changes with the time course of biological markers involved in stromal restructuring during neoplasia to further explain these results.

References

[1] K.I. Tosios, "Loss of basement membrane components laminin and type IV collagen parallels the progression of oral epithelial neoplasia," *Histopathology*, 1998; 30, pp. 15–64.

[2] S. Silverman, *Oral Cancer 3rd Ed.* Atlanta, 1990.

[3] J. Sun J, T. Shilagard, B. Bell, M Motamedi, G. Vargas, "In vivo multimodal nonlinear optical imaging of mucosal tissue," Optics Express, 2004; 12(11):2478-86.

[4] G.Vargas, T. Shilagard; J. Sun; M. Motamedi, "In vivo multiphoton and second harmonic generation microscopy of epithelial carcinogenesis," SPIE Proc. Vol. 6091

[5] Wilder-Smith P, Osann K, Hanna N, El Abbadi N, Brenner M, Messadi D, Krasieva T, In vivo multiphoton fluorescence imaging: a novel approach to oral malignancy, Lasers Surg Med, 2004; 35(2):96-103..

[6] M.C. Skala, J.M. Squirrell, K.M. Vrotsos, J.C. Eickhoff , A. Gendron-Fitzpatrick, K.W. Eliceiri, N. Ramanujam , "Multiphoton microscopy of endogenous fluorescence differentiates normal, precancerous, and cancerous squamous epithelial tissues," Cancer Res., 2005; 65(4):1180-1186..

[7] P.J. Campagnola, A.C. Millard, M. Terasaki, P.E. Hoppe, C.J. Malone, W.A. Mohler, "Three-dimensional high-resolution second-harmonic generation imaging of endogenous structural proteins in biological tissues," Biophys J. 2002; 82:493-508.

[8] A. Ebihara, T.B. Krasieva, L.H. Liaw, S. Fago, D. Messadi, K. Osann, P. Wilder-Smith, "Detection and diagnosis of oral cancer by light-induced fluorescence." Lasers in Surgery & Medicine, 2003; 32:17-24.

[9] A.M. Kluftinger, N.L. Davis, N.F. Quenville, S. Lam, J. Hung J, B. Palcic. "Detection of squamous cell cancer and precancerous lesions by imaging of tissue autofluorescence in the hamster cheek pouch model," Surgical Oncology, 1992; 1:183-188.

[10]